GEOPHYSICAL RESEARCH LETTERS, VOL. 33, L20703, doi:10.1029/2006GL027662, 2006

A precisely dated climate record for the last 9 kyr from three high alpine stalagmites, Spannagel Cave, Austria

Nicole Vollweiler,[1] Denis Scholz,[1] Christian Mühlinghaus,[1] Augusto Mangini,[1] and Christoph Spötl[2]

Received 26 July 2006; revised 8 September 2006; accepted 14 September 2006; published 24 October 2006.

[1] Here we use the $\delta^{18}O$ time-series of three stalagmites from the high alpine Spannagel cave (Austria) which grew in small distance from each other to construct a precisely dated, continuous $\delta^{18}O$ curve for the last 9 kyr (COMNISPA). This speleothem record is not influenced by effects of kinetic isotope fractionation due to the low temperatures in the cave. Thus, the variations in $\delta^{18}O$ can be interpreted in terms of past climate change. COMNISPA exhibits several oscillations within the Holocene, and their timing and duration is in agreement with that documented by other alpine archives. **Citation:** Vollweiler, N., D. Scholz, C. Mühlinghaus, A. Mangini, and C. Spötl (2006), A precisely dated climate record for the last 9 kyr from three high alpine stalagmites, Spannagel Cave, Austria, *Geophys. Res. Lett.*, *33*, L20703, doi:10.1029/2006GL027662.

1. Introduction

[2] The reconstruction of Holocene climate is mainly based on tree-ring chronologies [*Cook et al.*, 2002; *Büntgen et al.*, 2005; *Frank and Esper*, 2005], pollen data [*Lotter et al.*, 2000; *Davis et al.*, 2003] and high-resolution time-series from ice-cores [*Fischer et al.*, 1999], sediment cores [*Bond et al.*, 2001; *Haug et al.*, 2001], and stalagmites [*Neff et al.*, 2001; *Fleitmann et al.*, 2003; *Wang et al.*, 2005]. Most of these archives indicate a Northern Hemisphere climatic optimum during the Mid-Holocene between 9 and 6 thousand years ago (kyr) which is ascribed to the maximum in Northern summer insolation [*Berger and Loutre*, 1991]. Furthermore, several decadal to centennial climate oscillations like the Medieval Warm Period (MWP) are visible [*Moberg et al.*, 2005], but their trigger has remained uncertain so far [*Broecker*, 2001; *Mann and Jones*, 2003; *Luterbacher et al.*, 2004]. The compilation of *Mayewski et al.* [2004] revealed six periods of rapid climate change (RCC) of global extent and showed that Holocene climate has been highly variable. However, not all sites responded equally and synchronously during these events. Some of these mismatches may be attributed to dating uncertainties.

[3] The Alps belong to the regions where the Holocene climate variability has been most intensively studied. Variations in vegetation, glacier extension [*Nicolussi and Patzelt*, 2000; *Hormes et al.*, 2001; *Holzhauser et al.*, 2005; *Joerin et al.*, 2006], timberline [*Haas et al.*, 1998; *Tinner and Theurillat*, 2003], tree-ring width as well as periods of solifluction and pedogenesis and lake and river history [*Magny*, 2004; *Magny and Haas*, 2004] indicate major climate oscillations. A compilation of these results is given for example by *Furrer* [2001] and *Veit* [2002]. Accordingly, exceptionally warm conditions prevailed between 9 and 6, around 4, between 2.3 and 1.6 kyr (Roman Warm Period, RWP), and around 1 kyr (MWP). Cooler conditions are detected around 5.5, 3.3 and between 0.65 and 0.15 kyr (Little Ice Age, LIA).

[4] Stalagmites are ideally suited to investigate short-term Holocene climate variability because they can be precisely dated with U-series methods and record variations of past temperature and precipitation in their oxygen isotope signals with high resolution [e.g. *Neff et al.*, 2001; *Fleitmann et al.*, 2003]. Here we use three stalagmites from the high-alpine Spannagel cave (Austria) to construct a combined oxygen isotope record for the last 9 kyr which shows several distinct climate oscillations.

2. Geologic and Climatic Setting

[5] The Spannagel cave is located around 2,500 m above sea level (asl) at the end of the Tux Valley in Tyrol (Austria) close to the Hintertux glacier (auxiliary material[1] Figure S1). While the area above the cave is ice free at present, it was covered by ice during past glacials as well as during colder periods of Interglacials. It is important to note that the coverage of the cave by the glacier does not necessarily lead to a cessation of stalagmite growth as long as the glacier is temperate. *Spötl et al.* [2006] proposed that the area of Spannagel cave was covered by a temperate glacier during Marine Isotope Stage (MIS) 3 which was substantially colder than the Holocene. These conditions made possible stalagmite growth even during this colder period.

[6] Presently, the temperature inside the cave is between 1.8° and 2.0° C, and relative humidity is near 100%. The CO_2 concentration of cave air is similar to the corresponding atmospheric value at this altitude which is related to the sparse soil and vegetation cover above the cave system. As a consequence, the acidity required to dissolve the marble host rock is only partially derived from pedogenic CO_2; oxidation of disseminated sulfides also releases acid which reacts with the marble [*Holzkämper et al.*, 2005]. Therefore, the $\delta^{13}C$ signals in these stalagmites are affected by site specific factors [*Spötl et al.*, 2004; *Holzkämper et al.*, 2005; *Spötl et al.*, 2006]. From this follows that the $\delta^{13}C$ signals of the speleothems provide

[1] Heidelberger Akademie der Wissenschaften, Heidelberg, Germany.
[2] Institut für Geologie und Paläontologie, Leopold-Franzens-Universität Innsbruck, Innsbruck, Austria.

0094-8276/06/2006GL027662$05.00

[1] Auxiliary material data sets are available at ftp://ftp.agu.org/apend/gl/2006gl027662. Other auxiliary material files are in the HTML.

minor information on climate related soil processes and are difficult to interpret. Thus, it is not possible to complement the interpretation of δ^{18}O by δ^{13}C.

3. Material and Methods

[7] The three Holocene stalagmites used in this study (SPA 12, SPA 128, and SPA 70) were collected far from the cave entrance in the so-called "Tropfsteingang" (auxiliary material Figure S1). While SPA 12 (2,347 m asl) and SPA 128 (2,344 m asl) grew closely to each other (8–10 m distance), stalagmite SPA 70 (2,335 m asl) was sampled in a distance of approximately 50 m. Thus, all three stalagmites formed under very similar conditions.

[8] The three stalagmites were dated with the U/Th-method. The sample preparation and U/Th-measurements are described in detail in the auxiliary material. U/Th dating results are listed in auxiliary material Table S1. All ages are quoted as kyr ago and correspond to the year of measurement (i.e., 2004 AD). A conversion to kyr BP can be performed by subtracting 54 yr. Samples for stable oxygen isotope analysis were measured by mass spectrometry (see auxiliary material).

4. Results

[9] Auxiliary material Figure S2 shows the age-depth-relationships for all three stalagmites. Sample SPA 12 grew within the last 5 kyr. The younger part (between 0 and 15 cm distance from top) with a rather high growth rate (75 μm/yr) was already used to derive a temperature reconstruction for the last 2 kyr [*Mangini et al.*, 2005]. The older section (between 15 and 20 cm distance) exhibits a substantially slower growth rate (17 μm/yr). Stalagmite SPA 128 covers the period between 5.5 and 2.5 kyr and shows a rather constant growth rate (40 μm/yr) except for its oldest part between 8.5 and 10.5 cm distance from top. In this part which corresponds to a period between 5.5 and 4.6 kyr the growth rate was substantially slower indicating a possible hiatus (auxiliary Figure S2). Sample SPA 70 formed between 9.8 and 2.3 kyr with a constant growth rate of approximately 28 μm/yr. Similar to SPA 128, the age-depth model of SPA 70 indicates a hiatus between 4.6 and 3.6 kyr.

[10] To convert the δ^{18}O vs. depth profiles into δ^{18}O vs. age profiles, we constructed an age-depth model by applying an *Akima* [1970] interpolation (auxiliary Figure S2). The δ^{18}O vs. age profiles of the three stalagmites are shown in auxiliary material Figure S3. δ^{18}O values in sections with possible hiatuses (auxiliary material Figure S2) are not displayed. Overall, the three stalagmites cover the last 9 kyr whereas the period between 9 and 5.5 kyr is only represented by sample SPA 70 and the last 2.5 kyr are only recorded by SPA 12. Between 5.5 and 2.5 kyr the three stalagmites grew simultaneously providing the potential to build a combined record from all three samples.

5. Constructing a Combined Record for the Last 9 kyr

[11] Because the three stalagmites were collected in the same passage of the cave within a maximum distance of 50 m, we expect that they all grew under similar environmental conditions. In principle, the oxygen isotope signal of speleothems is influenced by (i) the δ^{18}O of the drip water, (ii) the temperature in the cave, and (iii) effects of kinetic isotope fractionation [*Mickler et al.*, 2004, 2006]. Due to the very low (1.8–2°C) temperatures that are accompanied by high drip rates in summer, outgassing of excess CO_2 is very slow in the Spannagel cave, and kinetic effects should therefore be negligible (see auxiliary material for details and compare auxiliary material Figure S4) [*Hendy*, 1971; *Mickler et al.*, 2004; *Mangini et al.*, 2005; *Mickler et al.*, 2006]. The sampling sites are located deep inside the cave. Thus, and because of the small distance between the different sampling sites, we can reasonably assume that the overlapping growth periods of the stalagmites were affected by the same variations of temperature in the cave. Based on this, discrepancies in the δ^{18}O signals of the three speleothems should mainly result from differences in the δ^{18}O values of their drip water. It was shown for SPA 12 that the oxygen isotope composition of drip water lies on a mixing line of two different end-members, consisting of a northern precipitation component, characterised by low δ^{18}O values, and a southern component with higher values [*Mangini et al.*, 2005]. We expect all three stalagmites to be similarly influenced by these variations. The different levels of the oxygen isotope signals of the three speleothems, however, imply a contribution of a third component, for example melt water from the glacier. The generally lower δ^{18}O values of stalagmites SPA 128 and SPA 70 (auxiliary material Figure S3) may then be explained by a higher contribution of glacial melt water with low δ^{18}O values. Such variations may be caused by different flow paths of the seepage waters.

[12] To generate a combined record for the last 9 kyr with the three stalagmites, the differences in the levels of their δ^{18}O signals must be accounted for (auxiliary material Figure S3). We use the level of SPA 12 as a reference for the combined record because (i) it covers the most recent period and (ii) there is already a temperature reconstruction available based on these isotope data. Because the different δ^{18}O levels seem to be a general feature of the individual records (auxiliary material Figure S3), this can be corrected by adjusting the entire records of SPA 128 and SPA 70 on the level of SPA 12. Details of the construction are given in the auxiliary material. The combined δ^{18}O curve (COMNISPA, Figure 1) is composed of (i) the original SPA 12 record between 0.07 and 2.56 kyr, (ii) the averaged curve of SPA 12 and SPA 128 (adjusted to the level of SPA 12) between 2.56 and 4.62 kyr, (iii) the SPA 12 record between 4.62 and 5.07 kyr and (iv) the SPA 70 record (adjusted on the SPA 12 level) between 5.07 and 9 kyr.

[13] To account for possible uncertainties arising from the adjustment of the individual curves, an uncertainty range for the composite part of the curve was estimated (see auxiliary material) (Figure 1). Because the single parts of the COMNISPA record mainly consist of the δ^{18}O signal of an individual stalagmite, the error ranges rather give an estimate of the uncertainty of the absolute level of the combined signal than of the successive variations.

6. Discussion

[14] The combined δ^{18}O record of the three stalagmites shows substantial variability within the last 9 kyr (Figure 1),

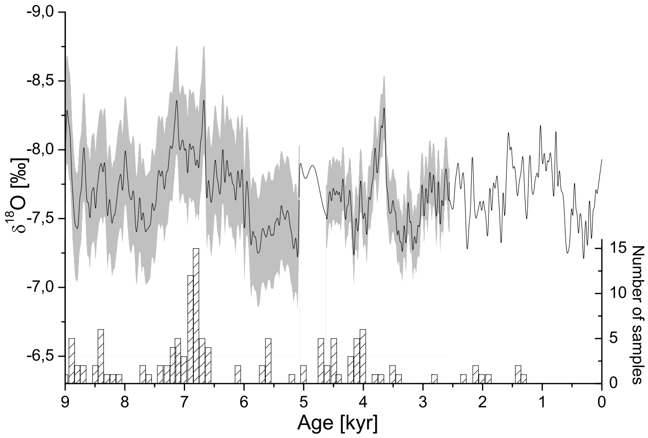

Figure 1. COMNISPA: the combined record derived from SPA 12, SPA 128 and SPA 70 (see text for details) in comparison with dated wood and peat samples indicating glacier extensions smaller than 1985 AD [*Joerin et al.*, 2006]. The grey areas indicate the uncertainty ranges for the composite parts of the curve (see text). COMNISPA exhibits substantial oscillations with low δ^{18}O values between 7.5 and 5.9 kyr (Holocene Climatic Optimum), 3.8 and 3.6, and 1.2 and 0.7 kyr (MWP) and high δ^{18}O between 7.9 and 7.5, 5.9 and 5, 3.5 and 3 kyr, and 600 and 150 yr (LIA). The timing and duration of these variations is in good agreement with that of warm periods documented by dated wood and peat samples [*Joerin et al.*, 2006] and other alpine archives.

characterized by short–term periodic events rather than consistent long-term trends. This supports the pollen-based results of *Davis et al.* [2003]. *Mangini et al.* [2005] provided two hydrological explanations for the observed relationship between climate and variability of δ^{18}O in the record of SPA 12 during the last 2 kyr. The first one relies on variable contributions of summer and winter precipitation to the ground water reservoir feeding the cave drip water. At present, winter precipitation contributes about 40%. A reduction of this value to 32% for instance, would result in δ^{18}O values higher by 1‰. The second explanation they provided is that the oxygen isotope composition of the stalagmites reflects changes of the strength of the NAO index which was shown to be related to temperature in the Alps [*Wanner et al.*, 2003]. For instance, a reduction of the contribution of isotopically lighter winter precipitation during a NAO+ situation would result in higher δ^{18}O values of the average annual precipitation and vice versa.

[15] According to this interpretation, the variations in isotopic composition result from mixing of different types of precipitation. *Mangini et al.* [2005] converted the δ^{18}O signal of stalagmite SPA 12 into temperature by applying a transfer function which is based on five points with reconstructed temperature and the δ^{18}O value in the corresponding sections of the stalagmite and published a temperature reconstruction for the last 2 kyr. The COMNISPA record presented here (Figure 1) may thus be interpreted as a temperature signal with low δ^{18}O values corresponding to warmer temperatures and high δ^{18}O values corresponding to colder temperatures. Application of the transfer function derived for SPA 12 would indicate values between 0 and 3.2° C over the last 9 kyr. However, this transfer function is based on values from the last 500 yr only, and we cannot take for granted that the conditions assumed by *Mangini et al.* [2005] hold for the whole Holocene. Furthermore, due to the variable contribution of meltwater from the glacier to the three speleothems, we do not calculate past temperatures from our record and focus on the fluctuations in δ^{18}O here.

[16] The COMNISPA record shows several periods of low and high δ^{18}O values, respectively, within the last 9 kyr (Figure 1). The most pronounced and long-lasting phase of low δ^{18}O values occurs between 7.5 and 6.5 kyr and persists on slightly higher values until 5.9 kyr. Further periods of low δ^{18}O values are between 3.8 and 3.6 kyr and during the MWP between 1.2 and 0.7 kyr. Between 2.25 and 1.7 kyr, a time known as the Roman Warm Period (RWP), some of the Alpine passes were ice-free also in winter [*Veit*, 2002]. COMNISPA shows higher δ^{18}O values during the RWP than during the MWP and suggests a shorter duration of the RWP than other archives (e.g., the glacier extension record, Figure 2). It is noteworthy, however, that COMNISPA has a pronounced peak at 2.2 kyr, synchronous with Hannibal‘s crossing of the Alps in 218 BC [*Veit*, 2002].

[17] In contrast, periods of high δ^{18}O are visible between 7.9 and 7.5, 5.9 and 5.1, 3.5 and 3 kyr, and during the LIA between 600 and 150 yr. The period between 5.9 and 5.1 kyr has equivalence in many records from various regions in both hemispheres corresponding to global cooling [*Magny and Haas*, 2004]. It also includes the time of the Alpine Iceman at 5.3 kyr [*Magny and Haas*, 2004].

[18] The timing of the climatic variations revealed by COMNISPA agrees approximately with that shown by other Alpine archives [*Haas et al.*, 1998; *Nicolussi and Patzelt*, 2000; *Hormes et al.*, 2001; *Magny*, 2004; *Magny and Haas*, 2004; *Mayewski et al.*, 2004; *Holzhauser et al.*, 2005].

[19] To minimize possible site specific differences between the records [*Mayewski et al.*, 2004], we compare COMNISPA only to alpine archives of glacier extension [*Holzhauser et al.*, 2005] and lake level [*Magny*, 2004] for the last 3.5 kyr, as well as to a glacier extension record based on radiocarbon dated wood and peat fragments [*Joerin et al.*, 2006] for the last 9 kyr.

[20] *Holzhauser et al.* [2005] compared the timing of successive phases of advance and retreat of the Great Aletsch glacier during the last 3.5 kyr with lake level time series from eastern France and the Swiss Plateau (Figure 2) and suggested a correspondence between the paleohydrological and paleoglaciological records. However, the authors also discuss some discrepancies that are visible in Figure 2. The comparison of COMNISPA with this paleohydrological and paleoglaciological set of data shows that phases of low δ^{18}O values correspond to periods of low lake level and glacier retreat (Figure 2). Conversely, high δ^{18}O values match with high lake levels and phases of glacier advance. This correspondence supports the relationship between δ^{18}O in the Spannagel cave stalagmites and hydrology suggested by *Mangini et al.* [2005]. The timing of the variations in COMNISPA which has a higher resolution than the glacier as well as the lake level record agrees well with both records during the last 1.5 kyr, where all archives clearly record both the LIA and the MWP. However, in the older section, between 3.5 and 1.5 kyr, COMNISPA rather

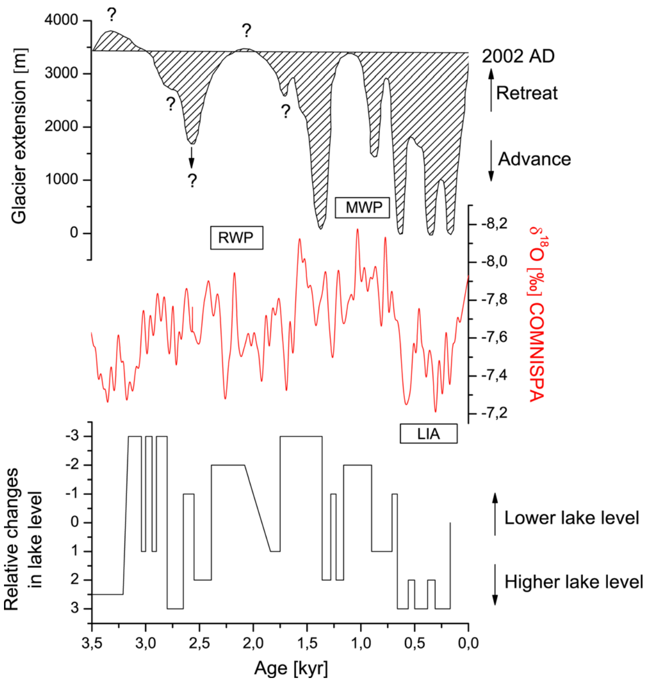

Figure 2. Comparison of COMNISPA (red) with the extension record of the Great Aletsch Glacier (Switzerland, top, after *Holzhauser et al.* [2005]) and the west-central European lake level record (bottom, after *Magny* [2004]) for the last 3.5 kyr. It is visible that glacier advances coincide with phases of higher lake level and vice versa in the majority of cases [*Holzhauser et al.*, 2005]. Several climatic oscillations recorded by COMNISPA are in good agreement with both records, for example during the Little Ice Age (LIA), the Medieval Warm Period (MWP), the phase between 1.6 and 1.4 and around 2.5 kyr. COMNISPA suggests a less pronounced Roman Warm Period (RWP) than the glacier extension record, but bears rather good resemblance to the lake level record. In the same way, COMNISPA and the lake level record have a rather high similarity between 3.5 and 3.2 kyr showing high δ^{18}O values and lake levels, respectively, while the glacier record suggests a lower extension than today.

agrees with the lake level record than with the glacier data. For example, the period of high lake level between 3.5 and 3.2 kyr corresponds to a period of higher δ^{18}O values in COMNISPA whereas it has no counterpart in the glacier record.

[21] *Joerin et al.* [2006] dated wood and peat samples which were released by melting Swiss Alpine glaciers located between Engadin and Valais. Figure 1 shows the age distribution of their samples indicating glacier extensions smaller than 1985 AD and, therefore, periods when climatic conditions were different than at this time [*Joerin et al.*, 2006]. Both the δ^{18}O maxima and minima recorded in COMNISPA clearly have counterparts in the glacier recession record [*Joerin et al.*, 2006]. In particular, the majority of wood and peat samples formed during the period between 7.3 and 6.5 kyr where COMNISPA exhibits its most pronounced phase of low δ^{18}O. Similarly, the δ^{18}O peak between 3.8 and 3.6 kyr has a counterpart around 4 kyr (Figure 1). Furthermore, there are no wood and peat samples from times of high δ^{18}O in COMNISPA (around 7.7, 5.3, and 3.2 kyr, Figure 1).

[22] Another interesting feature is that the prominent 8.2 kyr cold event (see *Alley and Ágústsdottir* [2005] for a detailed discussion), lasting from 8.3 to 8.1 kyr in COMNISPA, is not as pronounced as in other records. This indicates either that the 8.2 kyr event did not have such a strong impact in the Alps or that it is not reflected to its full extent in COMNISPA. This question cannot be answered at present. *Kofler et al.* [2005] analysed subfossil pollen in the Eastern Alps and found a vegetation response between 8.1 and 7.9 kyr suggesting cool summer temperatures. In addition, a moraine complex in the Silvretta Mountains, Austria, that was stabilized around 8.4 kyr may possibly be correlated with the 8.2 kyr event in a broader sense [*Kerschner et al.*, 2006]. In contrast, the alpine speleothem record from Grotta Savi [*Frisia et al.*, 2005] does not show a major 8.2 kyr event neither in δ^{18}O nor in δ^{13}C. Overall, the impact of the 8.2 kyr event has only rarely been demonstrated at high altitude sites yet, despite of its global character. Recently, *Ellison et al.* [2006] found that the 8.2 kyr event is marked by two distinct cooling events in the subpolar North Atlantic at 8.49 and 8.29 kyr. COMNISPA has two corresponding phases of high δ^{18}O values at 8.56 and 8.22 kyr, respectively, suggesting an impact, even though not as pronounced, and a similar timing of both events in the alpine region.

[23] In summary, despite some uncertainties in the interpretation of the δ^{18}O signal, COMNISPA represents a new high quality record for the Alpine Holocene with exceptionally small dating uncertainties and a resolution similar to that of ice cores. The records of lake level and glacier fluctuations in the Alpine region within the last 9 kyr reproduce to a good extent the COMNISPA reconstruction. Some of the discrepancies between the records could be due to different response time to climate forcing.

7. Conclusions

[24] We established a precisely dated, continuous δ^{18}O curve (COMNISPA) for the last 9 kyr based on three stalagmites from the high alpine Spannagel cave which grew in small distance from each other. Due to the low temperatures in the cave, they show negligible evidence for kinetic isotope fractionation. COMNISPA exhibits substantial oscillations with low δ^{18}O values between 7.5 and 5.9 kyr (Holocene Climatic Optimum), 3.8 and 3.6, and 1.2 and 0.7 kyr (MWP) and high δ^{18}O between 7.9 and 7.5, 5.9 and 5, 3.5 and 3 kyr, and 600 and 150 yr (LIA). The timing and duration of these variations reproduces to good extent the Alpine records of lake level [*Magny*, 2004] and glacier fluctuations [*Holzhauser et al.*, 2005] during the last 3.5 kyr. In addition, it is in agreement with the timing of periods of reduced glacier extension during the last 9 kyr documented by dated wood and peat samples [*Joerin et al.*, 2006]. This suggests that COMNISPA reflects past changes in both precipitation and temperature.

[25] **Acknowledgments.** We thank M. Wimmer and R. Eichstädter for their work in the stable isotope and TIMS laboratories. The manuscript was improved by two thoughtful anonymous reviews. The funding was

supplied by the DEKLIM program, FG 668 of the DFG (DAPHNE), and START Y122-GEO (FWF).

References

Akima, H. (1970), A new method of interpolation and smooth curve fitting based on local procedures, *J. ACM*, *17*, 589–602.

Alley, R. B., and A. M. Ágústsdottir (2005), The 8k event: Cause and consequences of a major Holocene abrupt climate change, *Quat. Sci. Rev.*, *24*, 1123–1149.

Berger, A., and M. F. Loutre (1991), Insolation values for the climate of the last 10 million years, *Quat. Sci. Rev.*, *10*, 297–317.

Bond, G., B. Kromer, J. Beer, M. Muscheler, N. Evans, W. Showers, S. Hoffmann, R. Lotti-Bond, I. Hajdas, and G. Bonani (2001), Persistent solar influence on North Atlantic climate during the Holocene, *Science*, *294*, 2130–2136.

Broecker, W. S. (2001), Was the Medieval Warm Period global?, *Science*, *291*, 1497–1499.

Büntgen, U., J. Esper, D. C. Frank, K. Nikolussi, and M. Schmidhalter (2005), A 1052-year tree-ring proxy for Alpine summer temperatures, *Clim. Dyn.*, *25*, 141–153.

Cook, E. R., R. D. D'Arrigo, and M. E. Mann (2002), A well-verified, multi-proxy reconstruction of the winter North Atlantic Oscillation since AD1400, *J. Clim.*, *15*, 1754–1765.

Davis, B. A. S., S. Brewer, A. C. Stevenson, and J. Guiot (2003), The temperature of Europe during the Holocene reconstructed from pollen data, *Quat. Sci. Rev.*, *22*, 1701–1716.

Ellison, C. R. W., M. R. Chapman, and I. R. Hall (2006), Surface and deep ocean interactions during the cold climate event 8200 years ago, *Science*, *312*, 1929–1932.

Fischer, H., M. Wahlen, J. Smith, D. Mastroianni, and B. Deck (1999), Ice core records of atmospheric CO_2 around the last three glacial terminations, *Science*, *283*, 1712–1714.

Fleitmann, D., S. J. Burns, M. Mudelsee, U. Neff, J. Kramers, A. Mangini, and A. Matter (2003), Holocene forcing of the Indian monsoon recorded in a stalagmite from Southern Oman, *Science*, *300*, 1737–1739.

Frank, D., and J. Esper (2005), Temperature reconstructions and comparisons with instrumental data from a tree-ring network for the European Alps, *Int. J. Climatol.*, *25*, 1437–1454.

Frisia, S., A. Borsato, C. Spötl, I. M. Villa, and F. Cucchi (2005), Climate variability in the SE Alps of Italy over the past 17,000 years reconstructed from a stalagmite record, *Boreas*, *34*, 445–455.

Furrer, G. (2001), *Alpine Vergletscherung vom letzten Hochglazial bis heute*, 49 pp., Franz Steiner Verlag, Stuttgart, Vienna.

Haas, J. N., I. Richoz, W. Tinner, and L. Wick (1998), Synchronous Holocene climatic oscillations recorded on the Swiss Plateau and at the timberline in the Alps, *Holocene*, *8*, 301–309.

Haug, G. H., K. A. Hughen, D. M. Sigman, L. C. Peterson, and U. Röhl (2001), Southward migration of the Intertropical Convergence Zone through the Holocene, *Science*, *293*, 1304–1308.

Hendy, C. H. (1971), The isotopic geochemistry of speleothems: I. The calculation of the effects of different modes of formation on the isotopic composition of speleothems and their applicability as palaeoclimatic indicators, *Geochim. Cosmochim. Acta*, *35*, 801–824.

Holzhauser, H., M. Magny, and H. J. Zumbühl (2005), Glacier and lake level variations in west-central Europe over the last 3,500 years, *Holocene*, *15*, 789–801.

Holzkämper, S., C. Spötl, and A. Mangini (2005), High-precision constraints on timing of Alpine warm periods during the middle to late Pleistocene using speleothem growth periods, *Earth Planet. Sci. Lett.*, *236*, 751–764.

Hormes, A., B. U. Müller, and C. Schlüchter (2001), The Alps with little ice: Evidence for eight Holocene phases of reduced glacier extent in the Central Swiss Alps, *Holocene*, *11*, 255–265.

Joerin, U. E., T. F. Stocker, and C. Schlüchter (2006), Multicentury glacier fluctuations in the Swiss Alps during the Holocene, *Holocene*, *16*, 697–704.

Kerschner, H., A. Hertl, G. Gross, S. Ivy-Ochs, and P. W. Kubik (2006), Surface exposure dating of moraines in the Kromer valley (Silvretta Mountains, Austria)—Evidence for glacial response to the 8.2 ka event in the Eastern Alps?, *Holocene*, *16*, 7–15.

Kofler, W., V. Krapf, W. Oberhuber, and S. Bortenschlager (2005), Vegetation responses to the 8200 cal. BP cold event and to long-term climatic changes in the Eastern Alps: Possible influence of solar activity and North Atlantic freshwater pulses, *Holocene*, *15*, 779–788.

Lotter, A. F., H. J. B. Birks, U. Eicher, W. Hofmann, J. Schwander, and L. Wick (2000), Younger Dryas and Allerod summer temperatures at Gerzensee (Switzerland) inferred from fossil pollen and cladoceran assemblages, *Paleogeogr. Paleoclimatol. Paleoecol.*, *159*, 349–361.

Luterbacher, J., D. Dietrich, E. Xoplaki, M. Grosjean, and H. Wanner (2004), European seasonal and annual temperature variability, trends, and extremes since 1500, *Science*, *303*, 1499–1503.

Magny, M. (2004), Holocene climate variability as reflected by mid-European lake-level fluctuations and its probable impact on prehistoric human settlements, *Quat. Int.*, *113*, 65–79.

Magny, M., and J. N. Haas (2004), A major widespread climatic change around 5300 cal. yr BP at the time of the Alpine Iceman, *J. Quat. Sci.*, *19*, 423–430.

Mangini, A., C. Spötl, and P. Verdes (2005), Reconstruction of temperature in the Central Alps during the past 2000 yr from a δ^{18}O stalagmite record, *Earth Planet. Sci. Lett.*, *235*, 741–751.

Mann, M. E., and P. D. Jones (2003), Global surface temperatures over the past two millennia, *Geophys. Res. Lett.*, *30*(15), 1820, doi:10.1029/2003GL017814.

Mayewski, P. A., et al. (2004), Holocene climate variability, *Quat. Res.*, *62*, 243–255.

Mickler, P. J., J. L. Banner, L. Stern, Y. Asmerom, R. L. Edwards, and E. Ito (2004), Stable isotope variations in modern tropical speleothems: Evaluating equilibrium vs. kinetic isotope effects, *Geochim. Cosmochim. Acta*, *68*, 4381–4393.

Mickler, P. J., L. A. Stern, and J. L. Banner (2006), Large kinetic isotope effects in modern speleothems, *GSA Bull.*, *118*, 65–81.

Moberg, A., D. M. Sonechkin, K. Holmgren, N. M. Datsenko, and W. Karlén (2005), Highly variable Northern Hemisphere temperatures reconstructed from low- and high-resolution proxy data, *Nature*, *433*, 613–617.

Neff, U., S. J. Burns, A. Mangini, M. Mudelsee, D. Fleitmann, and A. Matter (2001), Strong coherence between solar variability and the monsoon in Oman between 9 and 6 kyr ago, *Nature*, *411*, 290–293.

Nicolussi, K., and G. Patzelt (2000), Discovery of early-Holocene wood and peat on the forefield of the Pasterze Glacier, Eastern Alps, Austria, *Holocene*, *10*, 191–199.

Spötl, C., A. Mangini, S. J. Burns, N. Frank, and R. Pavuza (2004), Speleothems from the high-alpine Spannagel cave, Zillertal Alps (Austria), in *Studies of Cave Sediments: Physical and Chemical Records of Paleoclimate*, edited by I. D. Sasowsky, and J. Mylroie, pp. 243–256, Springer, New York.

Spötl, C., A. Mangini, and D. A. Richards (2006), Chronology and paleoenvironment of Marine Isotope Stage 3 from two high-elevation speleothems, Austrian Alps, *Quat. Sci. Rev.*, *25*, 1127–1136.

Tinner, W., and J.-P. Theurillat (2003), Uppermost limit, extent, and fluctuations of the timberline and treeline ecocline in the Swiss Central Alps during the past 11,500 years, *Arct. Antarct. Alp. Res.*, *35*, 158–169.

Veit, H. (2002), *Die Alpen - Geoökologie und Landschaftsentwicklung*, 352 pp., Verlag Eugen Ulmer, Stuttgart, Vienna.

Wang, Y., H. Cheng, R. L. Edwards, Y. He, X. Kong, Z. An, J. Wu, M. J. Kelly, C. A. Dykoski, and X. Li (2005), The Holocene Asian monsoon: Links to solar changes and North Atlantic climate, *Science*, *308*, 854–857.

Wanner, H., J. Luterbacher, C. Casty, R. Böhm, and E. Xoplaki (2003), Variabilität von Temperatur und Niederschlag in den europäischen Alpen seit 1500, in *Welt der Alpen - Gebirge der Welt*, edited by F. Jeanneret et al., pp. 61–76, Haupt, Bern, Switzerland.

A. Mangini, C. Mühlinghaus, D. Scholz, and N. Vollweiler, Heidelberger Akademie der Wissenschaften, Im Neuenheimer Feld 229, D-69120 Heidelberg, Germany. (nicole.vollweiler@iup.uni-heidelberg.de)

C. Spötl, Institut für Geologie und Paläontologie, Leopold-Franzens-Universität Innsbruck, Innrain 52, A-6020 Innsbruck, Austria.